Small noncoding RNA profiling across cellular and biofluid compartments and their implications for multiple sclerosis immunopathology

Galina Yurevna Zheleznyakova[a,1], Eliane Piket[a,1], Maria Needhamsen[a], Michael Hagemann-Jensen[b], Diana Ekman[c], Yanan Han[a], Tojo James[a,d,e], Mohsen Khademi[a], Faiez Al Nimer[a,f], Patrick Scicluna[a,b], Jesse Huang[a], Ingrid Kockum[a], Omid R. Faridani[b,g,h], Tomas Olsson[a,f], Fredrik Piehl[a,f], and Maja Jagodic[a,2]

[a]Department of Clinical Neuroscience, Karolinska Institutet, Center for Molecular Medicine, Karolinska University Hospital, SE-171 76 Stockholm, Sweden; [b]Department of Cell and Molecular Biology, Karolinska Institutet, SE-171 77 Stockholm, Sweden; [c]Department of Biochemistry and Biophysics, National Bioinformatics Infrastructure Sweden, Science for Life Laboratory, Stockholm University, SE-171 21 Stockholm, Sweden; [d]Department of Oncology-Pathology, Science for Life Laboratory, Karolinska Institutet, SE-171 21 Stockholm, Sweden; [e]Institute for Molecular Medicine Finland, Helsinki Institute of Life Science, University of Helsinki, FI-00290 Helsinki, Finland; [f]Center of Neurology, Academic Specialist Center, Stockholm Health Services, SE-113 65 Stockholm, Sweden; [g]Lowy Cancer Research Centre, School of Medical Sciences, University of New South Wales, NSW 2052 Sydney, Australia; and [h]Garvan Institute of Medical Research, NSW 2010 Sydney, Australia

Edited by Lawrence Steinman, Stanford University School of Medicine, Stanford, CA, and approved March 1, 2021 (received for review June 6, 2020)

Multiple sclerosis (MS) is a chronic inflammatory demyelinating disease affecting the central nervous system (CNS). Small noncoding RNAs (sncRNAs) and, in particular, microRNAs (miRNAs) have frequently been associated with MS. Here, we performed a comprehensive analysis of all classes of sncRNAs in matching samples of peripheral blood mononuclear cells (PBMCs), plasma, cerebrospinal fluid (CSF) cells, and cell-free CSF from relapsing-remitting (RRMS, $n = 12$ in relapse and $n = 11$ in remission) patients, secondary progressive (SPMS, $n = 6$) MS patients, and noninflammatory and inflammatory neurological disease controls (NINDC, $n = 11$; INDC, $n = 5$). We show widespread changes in miRNAs and sncRNA-derived fragments of small nuclear, nucleolar, and transfer RNAs. In CSF cells, 133 out of 133 and 115 out of 117 differentially expressed sncRNAs were increased in RRMS relapse compared to remission and RRMS compared to NINDC, respectively. In contrast, 65 out of 67 differentially expressed PBMC sncRNAs were decreased in RRMS compared to NINDC. The striking contrast between the periphery and CNS suggests that sncRNA-mediated mechanisms, including alternative splicing, RNA degradation, and mRNA translation, regulate the transcriptome of pathogenic cells primarily in the CNS target organ.

multiple sclerosis | microRNAs | small noncoding RNAs

Multiple sclerosis (MS) is a leading cause of neurological disability in young adults, affecting more than 2.3 million people worldwide (1). The pathology of MS is characterized by the periodic disruption of the blood–brain barrier and infiltration of immune cells, including T cells, B cells, and macrophages, into the central nervous system (CNS), resulting in demyelination, neuro-axonal degeneration, and neurological deficits. Both genes and environment contribute to disease risk; however, the exact molecular mechanisms that trigger MS are still unclear (2, 3).

Most MS patients (~85%) present with a relapsing-remitting (RRMS) disease course characterized by acute exacerbations, followed by periods of full or partial recovery (1). With time, more than half will convert to a stage of progressive worsening (i.e., secondary progressive MS [SPMS]). MS is diagnosed mainly based on its clinical manifestations, which are heterogeneous and not unique for MS (1). Both radiological and laboratory tests are therefore important to provide diagnostic specificity while easily measured molecular biomarkers are still largely lacking.

Small noncoding RNAs (sncRNAs) are important regulators of gene expression at the transcriptional and posttranscriptional level and consist of several classes that exert distinct and overlapping functions (4). The most investigated sncRNAs are microRNAs (miRNAs), which can regulate gene expression by binding to target messenger RNAs (mRNAs), leading to translational repression or mRNA degradation (5). Dysregulation of miRNAs has been described in a range of autoimmune diseases, suggesting involvement in underlying cellular immune mechanisms. Moreover, miRNAs packaged in extracellular vesicles can target gene expression in a recipient cell and thereby modulate immune reactions distally (6). Additionally, because of their stability in biofluids, miRNAs have been proposed as attractive biomarkers. Indeed, more than 60 studies have profiled miRNAs among different MS forms and treatments in a variety of biofluids and cellular compartments (7). The most consistently up-regulated miRNAs in MS include miR-142–3p ($n = 7$), miR-146a/b ($n = 11$),

Significance

Dysregulation of microRNAs (miRNAs), a type of small noncoding RNAs (sncRNAs), has frequently been associated with multiple sclerosis (MS). However, most studies have focused on peripheral blood, and few investigated other classes of sncRNAs. To address this, we analyzed all classes of sncRNAs in matching peripheral blood mononuclear cells, plasma, cerebrospinal fluid (CSF) cells, and cell-free CSF from MS patients and controls. We demonstrate widespread alterations of small nuclear (snRNA)–derived RNAs, small nucleolar-derived RNAs (sdRNAs), transfer RNA–derived fragments, and miRNAs, particularly in CSF cells. The striking contrast between the periphery and central nervous system and between relapse and remission phases of disease highlights the importance of sncRNA-mediated mechanisms in MS, in particular alternative splicing and mRNA translation.

Author contributions: G.Y.Z., E.P., and M.J. designed research; G.Y.Z., E.P., M.H.-J., M.K., F.A.N., P.S., T.O., and F.P. performed research; G.Y.Z., E.P., M.N., M.H.-J., D.E., Y.H., T.J., J.H., I.K., O.R.F., and M.J. analyzed data; G.Y.Z., E.P., M.N., and M.J. wrote the paper; D.E. and O.R.F. contributed analytical input; and M.K., F.A.N., T.O., and F.P. collected and managed samples and clinical information.

Competing interest statement: F.P. received research grants from Genzyme, Merck KGaA, and Novartis and fees for serving as chair of data monitoring committees in clinical trials with Parexel. T.O. received unrestricted MS research grants and honoraria for lectures or advisory boards from Biogen, Novartis, Sanofi, Merck, and Roche, none of which have relation to this work.

This article is a PNAS Direct Submission.

[1]G.Y.Z. and E.P. contributed equally to this work.

[2]To whom correspondence may be addressed. Email: maja.jagodic@ki.se.

This article contains supporting information online at https://www.pnas.org/lookup/suppl/doi:10.1073/pnas.2011574118/-/DCSupplemental.

Published April 20, 2021.

and miR-155 ($n = 12$), while family members of miR-15 ($n = 8$), miR-548 ($n = 7$), and let-7 ($n = 8$) exhibit down-regulation (the number of reporting studies is given in parenthesis) (7–11). These miRNAs have been implicated in immune processes including differentiation and function of $CD4^+$ T helper cells (12–14). Other miRNAs such as miR-150 and miR-181c, which are up-regulated in MS, have been proposed as biomarkers of different stages of disease, including early active MS (15, 16). However, studies profiling miRNAs using genome-wide approaches and that investigate other classes of sncRNAs are scarce (7).

Down-regulation of several small nucleolar RNAs (snoRNAs) has been reported in peripheral blood mononuclear cells (PBMCs), T cells, and plasma of MS patients (17–20). SnoRNAs are subdivided into the C/D box snoRNAs (SNORDs) that guide methylation of ribosomal RNA (rRNA) and H/ACA box snoRNAs (SNORAs) that assist in pseudouridylation of rRNA. In addition, snoRNAs have been implicated in chromatin remodeling, posttranscriptional gene silencing, splicing, and stress responses (21–23). They can be processed in shorter 17 to 24 nucleotide (nt) fragments of so-called snoRNA-derived RNAs (sdRNAs) that can exert miRNA-like functions and affect alternative splicing (21, 22, 24). Small Cajal body–associated RNAs (scaRNAs) represent a subset of snoRNAs that participate in the maturation of another class of sncRNAs (i.e., small nuclear RNAs [snRNAs]) that, in the form of ribonucleoprotein (U-snRNPs) complexes, are crucial components of the spliceosome. Increased levels of abnormally processed U1, U2, U4, U11, and U12 snRNAs, as well as Y1 RNA, have been described in mononuclear cells of RRMS patients (25). Y RNAs are components of Ro ribonucleoproteins, which are involved in DNA replication (26) and can release 22 to 36 nt Y RNA-derived small RNAs (ysRNAs) of yet unknown functions. Beyond their main role in translation, transfer RNAs (tRNAs) have been shown to be involved in various other processes, including cellular homeostasis and gene expression (27). Recent studies have investigated 13 to 35 nt tRNA-derived fragments (tRFs) as potential biomarkers in other diseases than MS (28, 29). Some of their roles include miRNA-like functions, involvement in rRNA biogenesis, and mRNA stability, as well as mediation of transgenerational effects (30, 31). Overall, studies investigating these sncRNA classes in the target CNS compartment in MS are still lacking.

Our objective was to perform a comprehensive sncRNA analysis in matching PBMCs, plasma, cerebrospinal fluid (CSF) cells, and cell-free CSF from MS patients and controls. To overcome issues related to the limited RNA input, particularly in CSF cells and cell-free CSF, we used the Small-seq method originally developed for single-cell analysis (32, 33). Our data demonstrate changes in several classes of sncRNAs, in particular, snRNAs-derived RNA fragments, sdRNAs, tRFs. and miRNAs, in MS patients. Moreover, we reveal distinct patterns of sncRNAs across different compartments of MS patients with important implications for their functional interpretation.

Results

Detection of sncRNAs. We utilized Small-seq (33), which incorporates unique molecular identifiers (UMIs) to quantify sncRNA transcripts (*SI Appendix*, Fig. S1*A*). Libraries were size selected before sequencing (*Materials and Methods* and *SI Appendix*, Fig. S2) and were analytically separated from potential precursor reads based on reads length of 18 to 40 nt (51 bp sequencing) (*SI Appendix*, Fig. S1*B*). Technical replication based on new libraries of three samples from each compartment demonstrated high reproducibility (*SI Appendix*, Fig. S4). As expected, the average percentage of aligned reads was higher in the cellular compartments compared to biofluids, with the lowest fraction observed in cell-free CSF (Fig. 1*A* and *SI Appendix*, Table S2 and Dataset S1), similar to previous reports (34, 35).

Considering the size distribution of detected sncRNAs, we classified unique RNA molecules into several categories: miRNA, tRF, sdRNA, and ysRNA as well as fragments derived from snRNA, mRNAs, ribosomal RNAs (rRNAs), long intergenic ncRNAs, and other sncRNAs (including mitochondrial transfer RNAs, vault RNAs, signal recognition particle RNAs, ribozymes, and miscellaneous RNAs) (Fig. 1 *B–D* and *SI Appendix*, Fig. S5). Transcripts mapping to the human genome that could not be annotated were classified as "unannotated" (Fig. 1*B*). The detected sncRNAs can represent full sncRNAs or be fragments actively derived from them. When sequencing CSF cells using longer read length (101 bp), we observed a small proportion of reads from miRNA precursors, full tRNAs, and full Y RNAs (Fig. 1*E* and *SI Appendix*, Fig. S2). On the other hand, a large proportion of reads from full snRNAs and snoRNAs was present (Fig. 1*E* and *SI Appendix*, Fig. S2).

Similar to other studies (35–38), we observed a distinct profile of sncRNA classes across cellular and biofluid compartments (Fig. 1 *B* and *C*). While miRNAs were the most abundant class of sncRNAs in PBMCs and plasma (26.4 and 27.9%, respectively), ysRNAs were dominant in plasma (29.6%), consistent with previous reports (36, 38). On the other hand, tRFs represented the most abundant class in CSF cells and cell-free CSF (43.6 and 30.3%, respectively), as previously suggested (35) (Fig. 1*B*). Thus, in addition to demonstrating high technical reproducibility over a range of samples with limited RNA input, Small-seq was concordant with previous studies in respect to the detected sncRNAs classes and their relative abundance.

Patterns of sncRNAs in MS Patients. Next, we investigated sncRNAs in PBMCs, plasma, CSF cells, and cell-free CSF samples from RRMS (relapse, $n = 12$ and remission, $n = 11$) and SPMS ($n = 6$) patients, as well as from noninflammatory and inflammatory neurological disease controls (NINDC, $n = 11$; INDC, $n = 5$) (*SI Appendix*, Table S1). We first focused on the comparison between RRMS and NINDC (Dataset S2), representing the groups of clinical interest with the largest number of individuals, while relatively small SPMS and INDC groups were only used for a group-level overview. We then compared the relapse phase of RRMS, characterized by recent worsening of symptoms and/or evidence of inflammatory activity in the CNS detected by imaging, with remission, a phase of stable symptoms without such signs (Dataset S3). An overview of the total number of detected sncRNAs for each class and compartment is summarized in Table 1, and the most abundant transcripts are provided in *SI Appendix*, Tables S3–S7.

Notably, while the majority of differentially expressed sncRNAs (adjusted [adj.] $P < 0.05$) were up-regulated in RRMS in the CSF compartment, they were down-regulated in PBMCs and plasma compared to NINDC (i.e., displaying an opposing pattern between the two compartments) (Fig. 2 *A* and *B*). In CSF cells, 115 out of 117 differentially expressed sncRNAs were up-regulated in RRMS, while in PBMCs 65 out of 67 differentially expressed sncRNAs were down-regulated compared to NINDC (Fig. 2*A*). Out of 65 sncRNAs down-regulated in PBMCs, 17 out of 25 tRFs and 2 out of 7 sdRNAs were significantly up-regulated in CSF cells in MS (Dataset S2). Comparison of RRMS relapse and remission showed a prominent mirroring pattern between these groups in general (Fig. 2*C*). Moreover, all of the 133 differentially expressed sncRNAs identified in CSF cells were up-regulated during relapse in RRMS patients, contrasting with a striking pattern of down-regulation in PBMCs (Fig. 2 *A* and *C* and Dataset S3). Although only one differentially expressed sncRNA was detected in plasma and none reached the significance threshold in cell-free CSF, the patterns generally followed changes observed in the respective cellular compartments (Fig. 2 *B* and *C*).

These observations suggest distinct sncRNAs patterns across different compartments in MS patients. In the following sections,

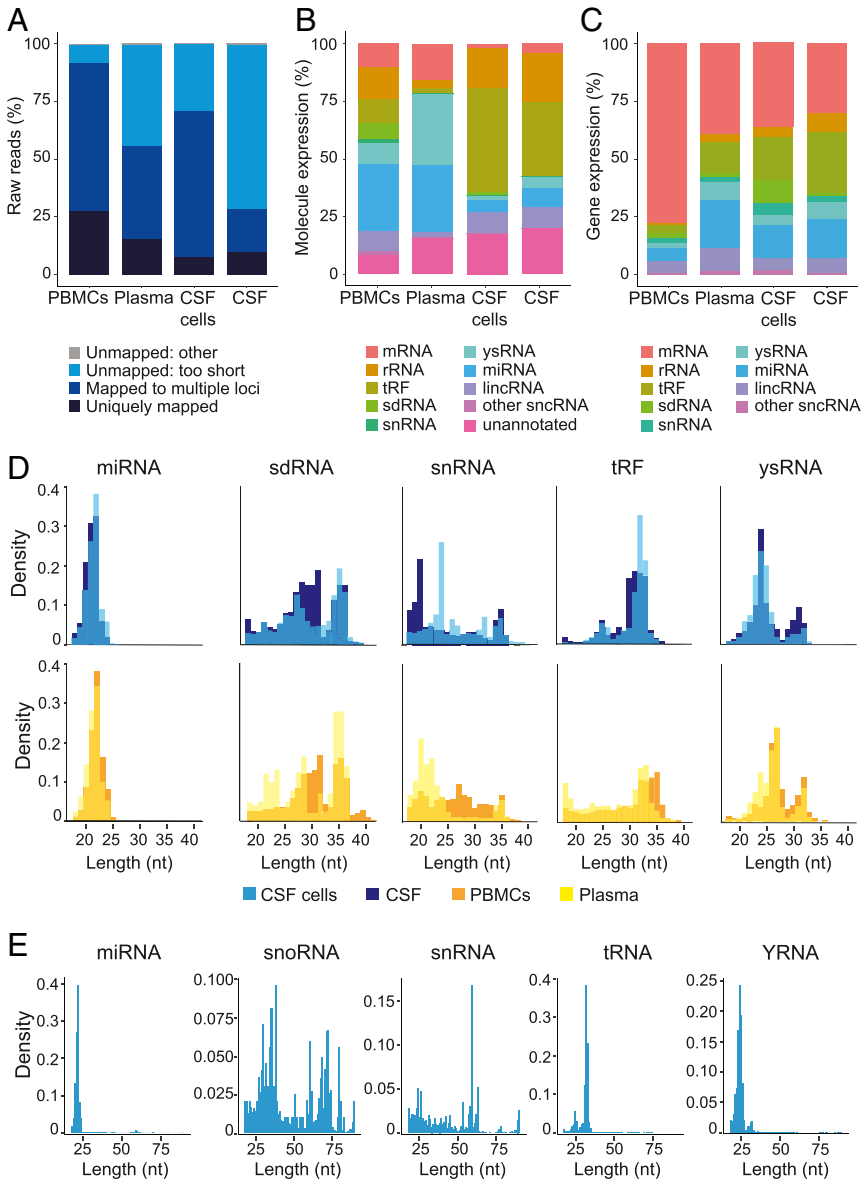

Fig. 1. Detection of sncRNAs. (*A*) Distribution of raw reads, (*B*) fraction of molecule (UMI) counts, and (*C*) fraction of genes expressed for different sncRNA classes across each cellular and biofluid compartment. Filtered (>2 UMI), raw molecule counts across all samples were used. Classes of sncRNAs include miRNAs and fragments derived from mRNAs, rRNAs, tRFs, sdRNAs, snRNAs, ysRNAs, long intergenic ncRNAs (lincRNA-derived), and other sncRNAs (fragments derived from mitochondrial transfer RNAs, vault RNAs, signal recognition particle RNAs, ribozymes, and miscellaneous RNAs). (*D*) Size distribution of sncRNAs in PBMCs, plasma, CSF cells, and cell-free CSF (51 bp read length). (*E*) Size distribution of sncRNAs in CSF cells (101 bp read length). See also *SI Appendix*, Figs. S2 and S5 and Table S2 and Dataset S1.

we present a detailed investigation of the most frequently differentially expressed sncRNAs. While we report only significant sncRNAs (adj. $P < 0.05$) in the following text, all sncRNAs with nominal $P < 0.01$ were included in heatmaps to investigate sncRNA patterns across patient groups and compartments (Figs. 3–5).

snRNA-Derived RNA Profile. We identified fragments derived from canonical snRNAs as well as "variant" snRNAs, which are encoded by pseudogenes of multiple snRNAs genes (39). Differentially expressed snRNA-derived fragments were detected only in the cellular compartments, likely because of their nuclear localization (Fig. 1*B*). In total, we identified 33 differentially expressed snRNA-derived fragments (adj. $P < 0.05$) in PBMCs between RRMS and NINDC, while in CSF cells, 19 were differentially expressed (adj. $P < 0.05$) between RRMS relapse and remission (Fig. 2*A* and Datasets S2 and S3).

Three distinct groups were distinguished based on their expression patterns across compartments (Fig. 3*A*). Members of the largest group comprised 31 snRNA-derived fragments (adj. $P < 0.05$) that were detected only in PBMCs and displayed down-regulation in RRMS compared to NINDC (Fig. 3*A* and Dataset S2). This group included fragments of canonical and variant/pseudogene transcripts of U1, U6 clusters, and U11 transcript. A second, smaller group, comprising fragments of two U1 transcripts (adj. $P < 0.05$), was also down-regulated in PBMCs of RRMS but displayed a clear opposing pattern of up-regulation in CSF cells compared to NINDC (Fig. 3*A*). The third and last group comprised 19 snRNA-derived fragments (adj. $P < 0.05$) that were up-regulated during RRMS relapse compared to remission in CSF

Table 1. Total number of detected sncRNA fragments in each class across four compartments

	PBMC	Plasma	CSF cells	CSF
RRMS versus NINDC analysis				
Total sncRNA fragments	1,673 (100%)	539 (100%)	469 (100%)	265 (100%)
miRNA	459 (27%)	212 (39%)	91 (19%)	62 (23%)
tRF	395 (24%)	157 (29%)	200 (43%)	120 (45%)
sdRNA	303 (18%)	8 (1%)	58 (12%)	0 (NA)
snRNA-derived	181 (11%)	25 (5%)	33 (7%)	1 (0%)
ysRNA	212 (13%)	82 (15%)	30 (6%)	30 (11%)
Other sncRNA	41 (2%)	13 (2%)	10 (2%)	1 (0%)
5S, 5.8S rRNA-derived	82 (5%)	42 (8%)	47 (10%)	51 (19%)
Relapse versus remission analysis				
Total sncRNA fragments	1,706 (100%)	617 (100%)	597 (100%)	334 (100%)
miRNA	475 (28%)	224 (36%)	117 (20%)	82 (25%)
tRF	395 (23%)	178 (29%)	227 (38%)	159 (48%)
sdRNA	308 (18%)	7 (1%)	93 (16%)	0 (NA)
snRNA-derived	188 (11%)	31 (5%)	44 (7%)	1 (0%)
ysRNA	217 (13%)	112 (18%)	42 (7%)	36 (11%)
Other sncRNA	40 (2%)	19 (3%)	16 (3%)	1 (0%)
5S, 5.8S rRNA-derived	83 (5%)	46 (7%)	58 (10%)	55 (16%)

A total number of detected sncRNA fragments in each class and number counted after the filtering threshold of two UMIs. Percentages represented by each sncRNA fragment class are shown in parenthesis after total numbers. NA, not available/detected.

cells but tended to be down-regulated in PBMCs (Fig. 3*A* and Dataset S3). Both canonical and pseudogene transcripts of the U2-1 cluster, U4, and U12, as well as the RN7SK transcript, belonged to this group.

To address whether snRNAs were present both as fragments and full-length snRNAs in CSF cells, we sequenced CSF cells using longer read length (101 bp) and performed differential expression analysis, which we compared with the original CSF cells sequencing data (51 bp). Longer read length indeed detected a proportion of reads from full snRNAs (Fig. 1*E* and *SI Appendix*, Fig. S2), which included a number of the differentially expressed snRNAs-derived fragments. U12, U4, and RN7SK were up-regulated in RRMS relapse compared to remission and showed a similar pattern to its corresponding full snRNAs (Datasets S4 and S5). This observation suggests that in addition to dysregulation of snRNA-derived fragments, it is likely that some of the full snRNAs are correspondingly dysregulated.

In summary, while U1/U6 transcripts were predominantly detected in PBMCs and showed down-regulation in RRMS compared to NINDC, U2 transcripts were more specific for disease activity with up-regulation in CSF cells and down-regulation in PBMCs in relapse compared to remission.

sdRNA Profile. Similar to snRNAs, due to their nucleolar localization sdRNAs were predominantly identified in cellular compartments (Fig. 1*B*). A total of 7 and 10 differentially expressed sdRNAs (adj. $P < 0.05$) were detected between RRMS and NINDC in PBMCs and CSF cells, respectively. We also identified 65 differentially expressed sdRNAs between RRMS relapse and remission in CSF cells (Fig. 2*A* and Datasets S2 and S3).

The differential expression profile in PBMCs and CSF cells separated sdRNAs into four distinct groups (Fig. 3*B*). The first group included 14 sdRNAs (adj. $P < 0.05$) that were up-regulated in RRMS relapse in CSF cells while displaying an opposing pattern of being down-regulated in PBMCs compared to remission (Fig. 3*B*, Dataset S3). The group contained sdRNAs that predominantly participate in modifications of 28S rRNA (*SI Appendix*, Table S5) and is represented by six H/ACA (including SNORA7A) and eight C/D box sdRNAs (such as SNORD69). Similar to the pattern in the first group, members of the second group, comprising 34 sdRNAs (adj. $P < 0.05$), were up-regulated in RRMS relapse compared to remission in CSF cells but, in contrast to the first group, displayed no clear differences in PBMCs (Fig. 3*B*). This group consisted predominantly of C/D box sdRNAs, including the *U22* locus sdRNAs (SNORD25 and SNORD27).

The third group comprised 17 sdRNAs (adj. $P < 0.05$) that were up-regulated in RRMS relapse compared to remission in CSF cells, similar to the first two groups (Fig. 3*B* and Dataset S3). They all showed a clear pattern of up-regulation in RRMS compared to NINDC in CSF cells, with 9 out of 17 being significantly different (adj. $P < 0.05$). However, they displayed an opposing pattern in PBMCs reflecting predominant down-regulation in RRMS compared to NINDC, with 5 out of 17 displaying significant difference (adj. $P < 0.05$). This group comprised C/D box sdRNAs, including another two *U22* locus sdRNAs (SNORD26 and SNORD30) and two H/ACA box sdRNAs (SNORA73A and SNORA73B). The last and fourth group was only expressed in PBMCs and exhibited the same pattern as the previous group, including C/D box sdRNA SNORD23 and SCARNA6 (adj. $P < 0.05$) that were down-regulated in RRMS compared to NINDC (Fig. 3*B* and Dataset S2).

To address whether snoRNAs were present both as fragments and full-length snoRNAs in CSF cells, we compared the longer read length (101 bp) with the original CSF cells sequencing data (51 bp). We observed a large proportion of full snoRNA reads in CSF cell libraries using longer read length (Fig. 1*E* and *SI Appendix*, Fig. S2). A large fraction of differentially expressed sdRNAs demonstrated a similar pattern of change for the corresponding full snoRNAs (Datasets S4 and S5). This suggests that what we observe likely represents dysregulation of both full snoRNAs as well as their fragments.

Thus, the vast majority of differentially expressed sdRNAs and snoRNAs were up-regulated in CSF cells from RRMS patients, specifically during the relapse phase, while the same sdRNAs and snoRNAs were frequently down-regulated compared to NINDC controls in PBMCs.

tRF Profile. Contrary to snRNAs and snoRNAs, we detected fragments of tRNAs almost exclusively (i.e., tRFs) (Fig. 1 *D* and *E*). We detected 25 and 91 differentially expressed tRFs (adj. $P < 0.05$) between RRMS and NINDC in PBMCs and CSF cells, respectively (Fig. 2*A* and Dataset S2). In total, 10 tRFs displayed differential expression (adj. $P < 0.05$) between RRMS relapse and remission in CSF cells (Fig. 2*A* and Dataset S3). For further

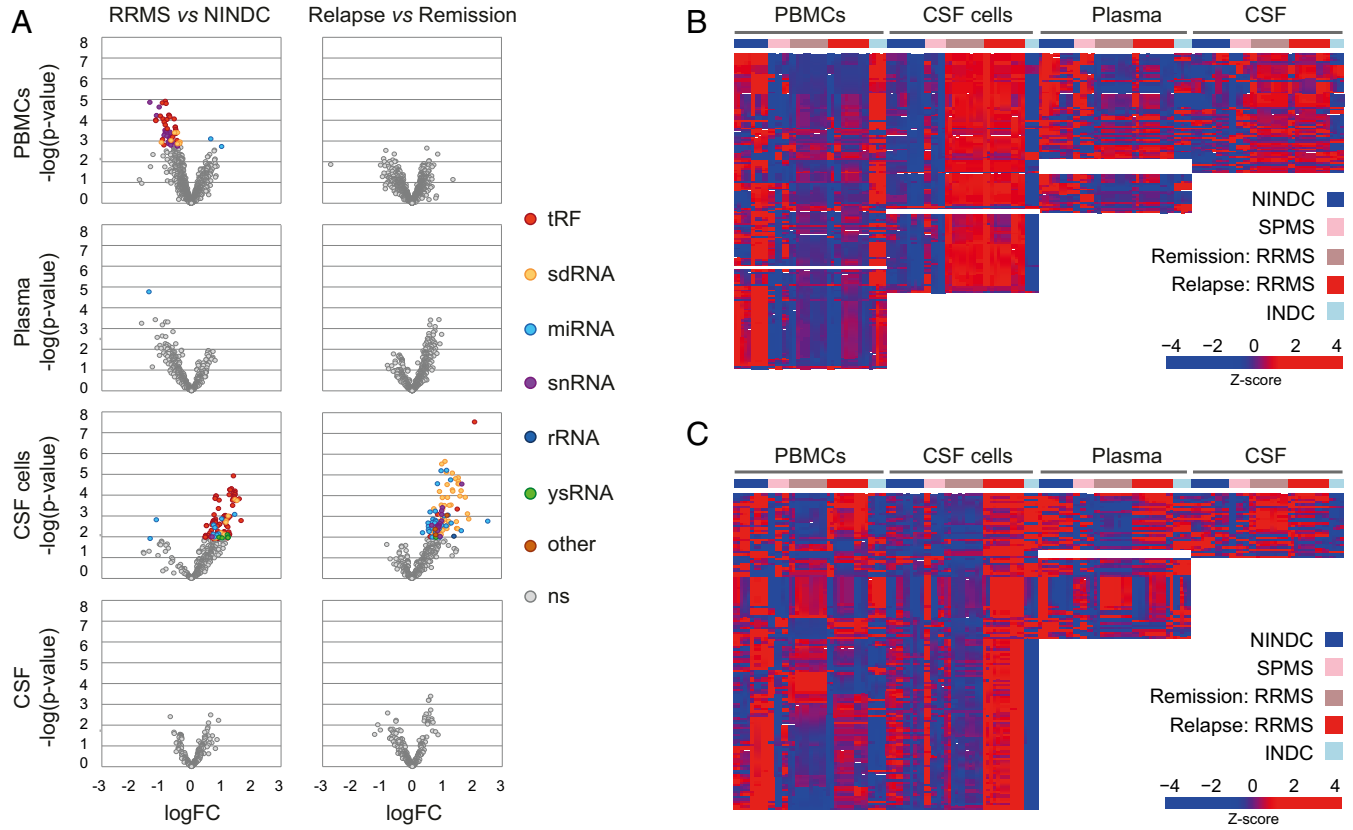

Fig. 2. sncRNA fragments associating with MS status and phase across four compartments. SncRNAs in PBMCs, CSF cells, plasma, and cell-free CSF from RRMS ($n = 12$ in relapse, $n = 11$ in remission), SPMS ($n = 6$), NINDC ($n = 11$) and INDC ($n = 5$). (*A*) Volcano plots illustrate differences in classes of sncRNAs, depicted in different colors, between RRMS versus NINDC and relapse versus remission. The *y*- and *x*-axes depict $-\log_{10}$(*P* value) and $\log_2$(fold-change), respectively. Colored circles indicate significant sncRNAs (adj. *P* value < 0.05); miRNAs and fragments of rRNA-derived, snRNA-derived, sdRNAs, tRFs, ysRNAs, and other sncRNAs (other); ns, not significant. Heatmaps of sncRNAs between (*B*) RRMS versus NINDC and (*C*) relapse versus remission (adj. *P* value < 0.05). Normalized Z-score (fitted log2-transformed UMI counts per million [lcmp]) values were centered and scaled for each compartment separately, with relative high levels illustrated in red, low levels in blue, and intermediate in purple (see color key). Row-wise hierarchical clustering was conducted based on RRMS-derived transcripts in PBMCs or CSF cells after subclustering NAs (white block), representing transcripts that did not pass the filtering threshold. Column-wise hierarchical clustering was conducted separately within each compartment and patient group.

analysis, we grouped tRFs based on their amino acid origin (*SI Appendix*, Fig. S5) and separated them into two main groups based on their differential expression patterns across compartments (Fig. 4*A*).

The first group of tRFs, coding for Lys, Glu, Pro, His, Ala, and Arg, was characterized by strong dysregulation between RRMS and NINDC and a contrasting pattern between CSF cells and PBMCs (Fig. 4*A*). A total of 19 Lys tRFs (both TTT and CTT isoacceptors) were up-regulated in RRMS (adj. $P < 0.05$) in CSF cells, most of them (17 out of 19) displaying down-regulation compared to NINDC in PBMCs (Fig. 4*A* and Dataset S2). In addition, 10 Glu (both CTC and TTC isoacceptors), 11 Pro (all isoacceptors), 3 His (GTG), and 4 Ala (TGC, CGC, AGC) tRFs were elevated in RRMS compared to NINDC (adj. $P < 0.05$) in CSF cells. In contrast, the vast majority of aforementioned tRFs displayed a clear trend for down-regulation in RRMS compared to NINDC in PBMCs (Fig. 4*A* and Dataset S2). Several of the Lys, Glu, and Pro tRFs were also detected in cell-free CSF and plasma, where their pattern mirrored the corresponding cellular compartments (i.e., CSF cells and PBMCs) (Fig. 4*A* and Dataset S2).

The second group of tRFs, coding for Met, Cys, Gly, and Val, displayed significant differential expression only in CSF cells (Fig. 4*A* and Dataset S2). The levels of 9 Met tRFs (involved in initiation and elongation) were significantly higher in RRMS compared to NINDC (adj. $P < 0.05$). Additionally, 5 Cys, 13 Gly (GCC, TCC, and CCC isoacceptors), and 16 Val (all isoacceptors) tRFs displayed the same pattern of up-regulation in RRMS compared to NINDC in CSF cells (adj. $P < 0.05$). Several of the Gly and Val tRFs were also detected in cell-free CSF, where their pattern mirrored the pattern in CSF cells (Fig. 4*A* and Dataset S2).

Considering that we almost exclusively detected tRFs, we used MINTmap (40) to further analyze tRFs, which map exclusively to the "tRNA space." In total, 7,894, 5,803, 2,454, and 2,845 tRFs were detected in PBMCs, plasma, CSF cells, and CSF, respectively, with the tRF length distribution varying across compartments (*SI Appendix*, Fig. S7*A*). MINTmap annotated five different tRF subtypes: 5′-half, 5-tRFs, i-tRFs, 3′-tRFs, and 3′-half. PBMCs, plasma, and cell-free CSF displayed similar tRF subtype distribution with 3′-tRFs being the most abundant (Fig. 4*B*). CSF cells were, on the other hand, predominantly composed of 5′-half tRFs, while 3′-half tRFs were rare in all compartments (Fig. 4*B* and *SI Appendix*, Fig. S7*B*). We have further investigated tRF composition using MINTmap for the most significantly changed tRFs found previously in CSF cells and PBMCs (Fig. 4 *C* and *D*). A similar tRF composition profile was observed for the differently expressed Met and Lys tRF isodecoders in CSF cells (Fig. 4*C*). Interestingly, the eight significantly dysregulated Lys tRFs in PBMCs represented three different tRF profiles (Fig. 4*D*).

Taken together, differentially expressed tRFs were particularly enriched in CSF cells and displayed extensive up-regulation in

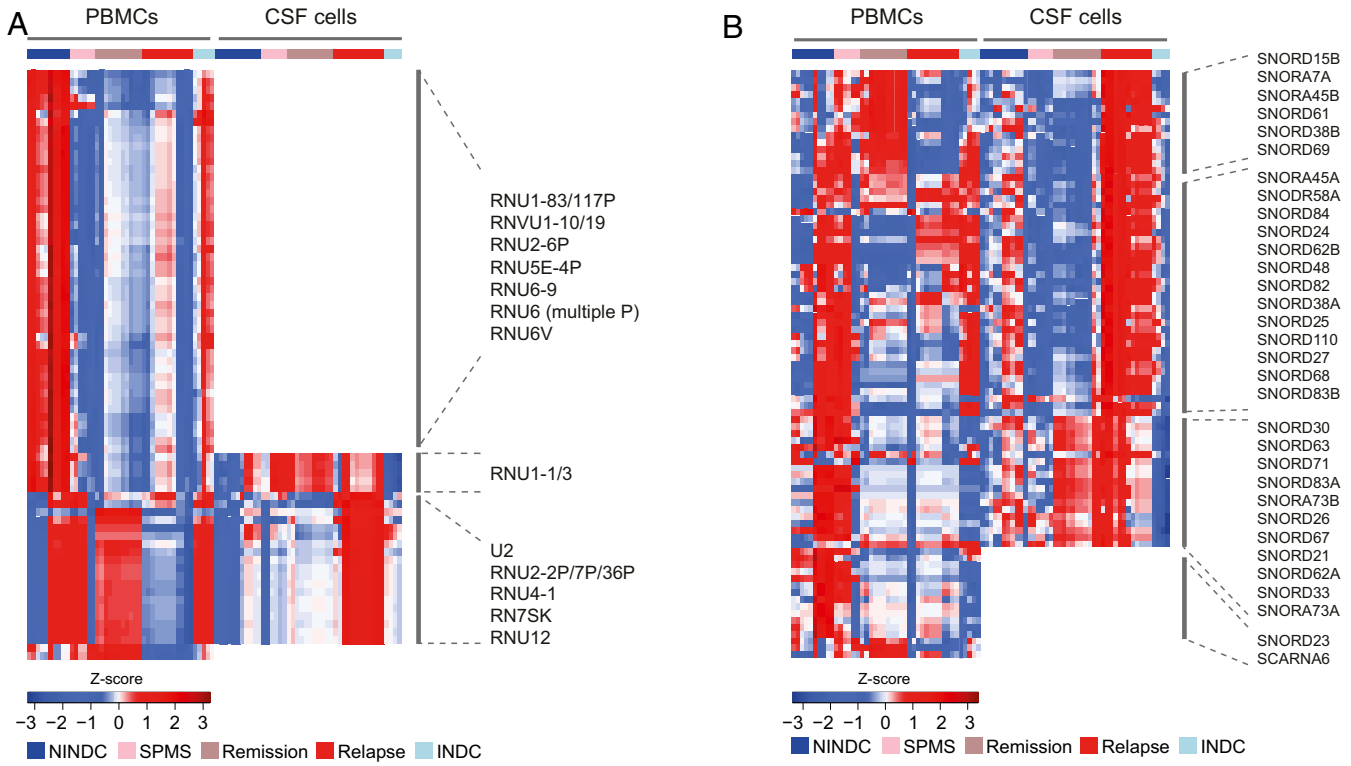

Fig. 3. snRNA- and snoRNA-derived fragments associating with MS status and phase across intracellular compartments. Heatmaps of (*A*) snRNA-derived and (*B*) snoRNA-derived (sdRNA) fragments in PBMCs and CSF cells from RRMS ($n = 12$ in relapse, $n = 11$ in remission), SPMS ($n = 6$), NINDC ($n = 11$), and INDC ($n = 5$). Transcripts between RRMS versus NINDC and/or relapse versus remission ($P < 0.01$) were included. Distinct groups of snRNA-derived RNAs and sdRNAs are depicted by the vertical lines, and representative molecules to the right of each heatmap were differentiated based on their profile in PBMCs and CSF cells. Heatmaps contain normalized Z-score (fitted lcmp) values were centered and scaled for each compartment separately, with relatively high levels illustrated in red, low levels in blue, and intermediate in white (see color key). Row-wise hierarchical clustering was conducted based on PBMC and/or CSF cell RRMS-derived transcripts after subclustering NAs (white block), representing transcripts that did not pass the filtering threshold. Column-wise hierarchical clustering was conducted separately within each compartment and patient group.

RRMS patients compared to controls, which contrasted with their unchanged or down-regulated profile in PBMCs.

miRNA Profile. A total of 13 differentially expressed miRNAs (adj. $P < 0.05$) were detected between RRMS and NINDC: 10 in CSF cells, 2 in PBMCs, and 1 in plasma (Fig. 2*A* and Dataset S2). In addition, 33 miRNAs were differentially expressed (adj. $P < 0.05$) between relapse and remission in CSF cells of RRMS patients (Fig. 2*A* and Dataset S3).

Based on the miRNA expression profile across compartments, we differentiated two main groups of miRNAs (Fig. 5*A*). Members of the first group of miRNAs were differentially expressed between RRMS and NINDC across multiple compartments (Fig. 5*A* and Dataset S2). A set of 10 miRNAs within this group also differed in CSF cells (adj. $P < 0.05$), with miR-146a-5p, miR-148a-3p, miR-150–5p, miR-181a-5p, miR-29a/b-3p, and miR-342–3p being up-regulated, while miR-204–5p and miR-371a-3p were down-regulated in RRMS compared to NINDC. In PBMCs, two miRNAs, including miR-548o-3p, were significantly up-regulated (adj. $P < 0.05$) in RRMS compared to NINDC, with many other miRNAs showing the same trend (Fig. 5*A*). In contrast, plasma miRNAs displayed predominant down-regulation, with miR-215–5p being significantly down-regulated (adj. $P < 0.05$) in RRMS compared to NINDC (Fig. 5*A* and Dataset S2).

Members of the second group were predominantly up-regulated in the relapse phase in PBMCs, plasma, and, in particular, in CSF cells, where 33 miRNAs were significantly up-regulated in relapse compared to remission (adj. $P < 0.05$) (Fig. 5*A* and Dataset S3). This group included miR-125a-5p, miR-146a/b-5p, miR-150–5p, miR-155–5p, miR-181a-5p, miR-21–3p, and miR-320a, together with several members of the let-7 family, such as let-7a/d/f/i-5p. Interestingly, a subset of them, including miR-21–5p, miR-92a-3p and let-7 members, displayed an opposing pattern in cell-free CSF and CSF cells between relapse and remission (Fig. 5*A* and Dataset S3).

To explore the possible functional implications, we performed ingenuity pathway analysis (IPA) on predicted targets of the most frequently differentially expressed miRNAs (i.e., the 33 miRNAs in CSF cells that were up-regulated in RRMS relapse compared to remission). Many of the identified (adj. $P < 0.05$), immune-related pathways concerned activation of T and B cells, as well as cytokine and chemokine signaling, with transforming growth factor beta (TGF-β) signaling being the most significantly enriched pathway (Fig. 5*B*).

The miRNA profile thus underscores a general up-regulation of miRNAs in RRMS, particularly in CSF cells during the relapse phase, with possible implications for regulation of T and B cell activation and differentiation.

Other sncRNAs. We also observed changes in the expression level of other sncRNAs between RRMS and NINDC (Fig. 2*A* and Dataset S2). Additionally, significantly higher levels of signal recognition particle RNA transcript (RN7SL1), as well as RNA component of mitochondrial RNA processing enzyme complex (RNase MRP RNA) and mitochondrially encoded tRNA-Met–derived tRF were found in CSF cells during RRMS relapse compared to remission (adj. $P < 0.05$, Dataset S3).

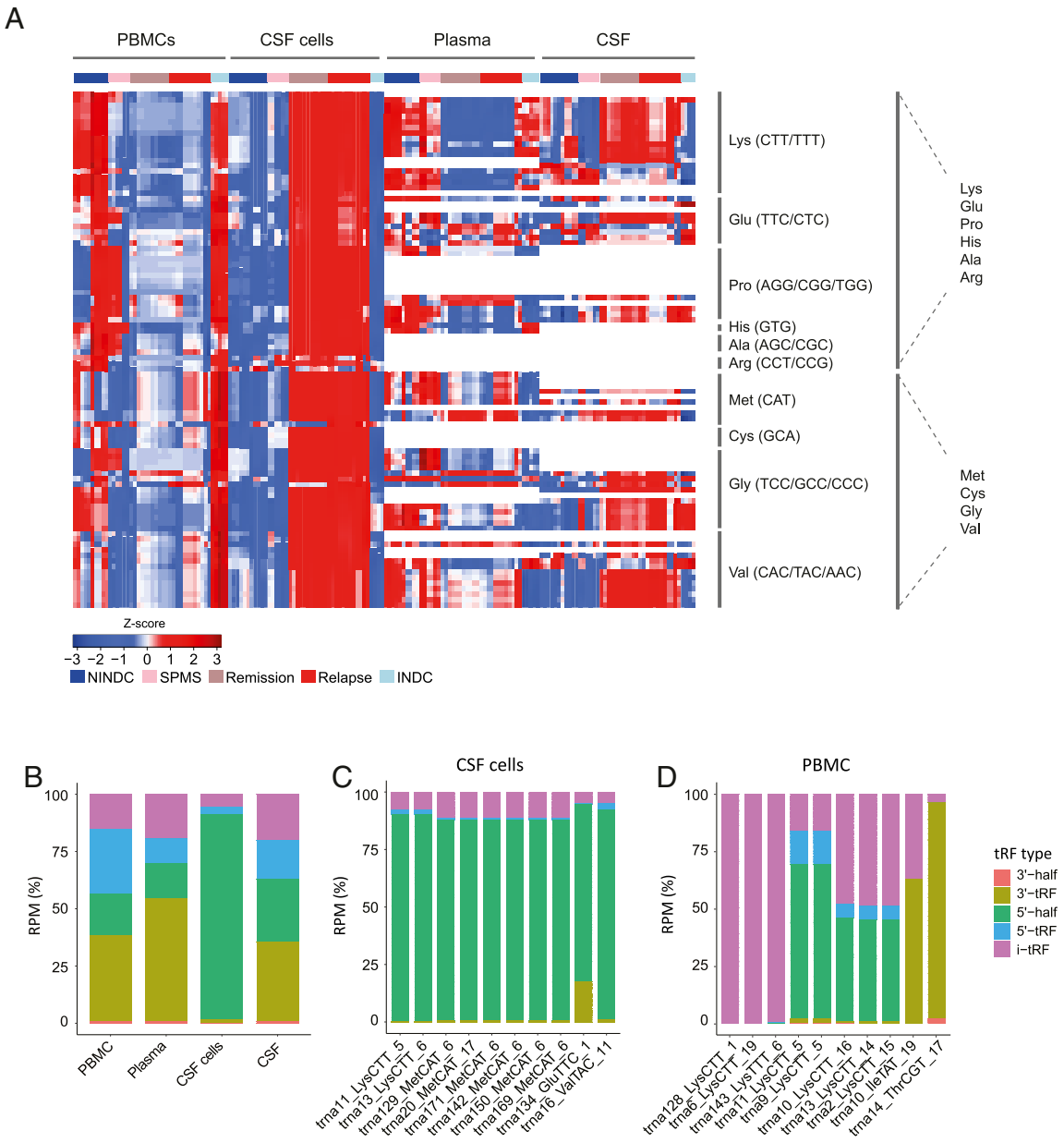

Fig. 4. tRFs associating with MS status and phase across four compartments. (*A*) Heatmap of tRFs in PBMCs, plasma, CSF cells, and cell-free CSF from RRMS ($n = 12$ in relapse, $n = 11$ in remission), SPMS ($n = 6$), NINDC ($n = 11$) and INDC ($n = 5$). Selected transcripts between RRMS versus NINDC and/or relapse versus remission (P value < 0.01) in PBMCs and CSF cells were included. tRFs were grouped based on amino acid origin, depicted by vertical lines with representative amino acid and tRNA anticodon(s) to the right of the heatmap. Two distinct groups of tRFs, depicted by second vertical lines and representative amino acid to the right of the heatmap, were differentiated based on the tRF profile in PBMCs and CSF cells. The heatmap contains normalized Z-score (fitted lcmp) values that were centered and scaled for each compartment separately, with relatively high levels illustrated in red, low levels in blue, and intermediate in white (see color key). Row-wise hierarchical clustering was based on PBMC and CSF cell compartments after subclustering based on amino acid origin. NAs (white block) represent transcripts that did not pass the filtering threshold. Column-wise hierarchical clustering was conducted separately within each compartment and patient group. (*B*) Distribution of different tRF subtypes was as follows: 5′-half, 5′-tRFs, i-tRFs, 3′-tRFs, and 3′-half, annotated using MINTmap. Reads per million (RPM) counts across all samples were used to analyze the distribution of different tRF subtypes in each compartment. See also *SI Appendix*, Fig. S7. (*C*) tRF subtype composition for the 10 most significantly dysregulated tRFs in CSF cells between RRMS and NINDC. (*D*) tRF subtype composition for the 10 most significantly dysregulated tRNAs in PBMC between RRMS and NINDC.

Biological Functions Implicated by Changes in Protein-Coding RNAs. In addition to sncRNAs, we investigated mRNA changes in CSF cells in a subgroup of individuals, 11 RRMS (relapse = 7 and remission = 4) and NINDC ($n = 6$), from the same cohort by total RNA sequencing (Dataset S6). To get an overview of biological functions associated with dysregulated transcripts, we conducted IPA analysis. Top significantly enriched canonical pathways between RRMS and NINDC include eukaryotic translation initiation factor 2 (EIF2) signaling, regulation of eIF4 and p70S6K signaling and mammalian target of rapamycin (mTOR) signaling, NRF2-mediated oxidative stress response, sirtuin signaling pathway and HIF1α signaling (Fig. 6*A*) with significantly enriched biological functions associated with protein synthesis, cell death and survival, cellular movement, and RNA damage and repair (Fig. 6*B*), among others. The same pathways and biological functions were confirmed using previously published transcriptome data from

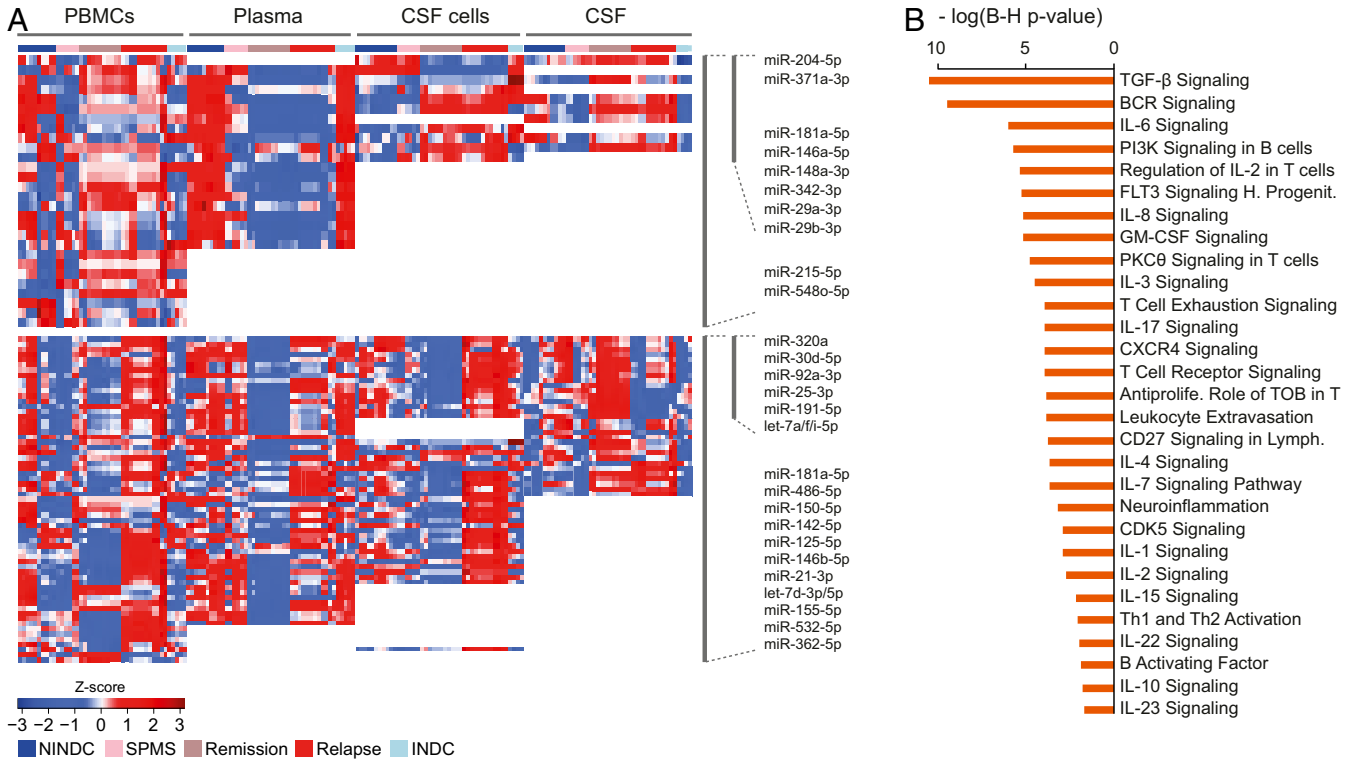

Fig. 5. miRNAs associating with MS status and phase across four compartments. (*A*) Heatmap of miRNAs in PBMCs, plasma, CSF cells, and cell-free CSF from RRMS (n = 12 in relapse, n = 11 in remission), SPMS (n = 6), and NINDC (n = 11) and INDC (n = 5). Transcripts between RRMS versus. NINDC and/or relapse versus remission (P value < 0.01) were included. Two distinct groups of miRNAs, depicted by the vertical lines and representative molecules to the right of the heatmap, were differentiated based on the miRNA profile across the compartments. The heatmap contains normalized Z-score (fitted lcmp) values, which were centered and scaled for each compartment separately, with relatively high levels illustrated in red, low levels in blue, and intermediate in white (see color key). Row-wise hierarchical clustering was conducted based on CSF, CSF cell, or PBMC RRMS-derived transcripts (relapse versus remission) after sub-clustering based on NAs (white block), representing transcripts that did not pass the filtering threshold. Column-wise hierarchical clustering was conducted separately within each compartment and patient group. (*B*) Significant immune-related canonical pathways (Benjamini–Hochberg-corrected P value < 0.05) generated using IPA on predicted target genes of miRNAs differentially expressed between relapse versus remission in CSF cells.

CSF cells from an independent larger cohort (41) of RRMS (n = 26) and NINDC (n = 18) patients (Fig. 6 *A* and *B*). Interestingly, there was a large overlap with biological pathways and functions enriched in mRNA fragments from PBMCs identified using Small-seq (*SI Appendix*, Fig. S8).

Moreover, levels of protein biomarkers measured in CSF (42) were correlated with sncRNA levels in CSF cells in overlapping samples (n = 22). Protein levels of eIF4E-binding protein 1 (4E-BP1) and stem cell factor (SCF), involved in several pathways mentioned above (EIF2 signaling, regulation of eIF4 and p70S6K signaling, and mTOR signaling) positively correlated with numerous Gly and Pro tRFs (Dataset S7). The highest correlations were observed between tRNA6-ProCGG_1 and 4E-BP1 and SCF (Fig. 6*C*).

Thus, additional evidence from protein-coding mRNA and protein analyses implicates sncRNAs in pathways associated with translation.

Discussion

We performed a comprehensive sncRNA analysis in blood and CNS compartments from matching samples of MS patients and controls utilizing Small-seq (32, 33). Our main findings demonstrate widespread alterations of several classes of sncRNAs, particularly during the relapse phase in CSF cells. Furthermore, we report an opposing pattern of snRNA, sdRNA, and tRF changes between the blood and CNS compartments. The patterns across several sncRNA species implicate changes in the general cellular mechanisms, such as alternative splicing and mRNA translation, occurring, for example, during lymphocyte activation, while cytokine signaling pathways critical for T helper differentiation were more selectively modulated by miRNAs. Collectively, these observations underscore the relevance of studying the CSF compartment in a CNS disease such as MS, with CSF reflecting more closely disease processes occurring in the target organ (43), including enrichment of encephalitogenic immune cell populations (44, 45).

We detected predominant up-regulation of snRNAs in CSF cells and down-regulation in PBMCs from RRMS patients compared to controls. We also observed increased levels of multiple U1, U2, U4, and U12 snRNA transcripts in CSF cells during the relapse phase. An altered level of U2-associated protein SR140 has previously been detected in CSF cells of MS patients compared to NINDC (41). Similar to our observations in PBMCs, diminished global levels of U1, U5, and U6 transcripts have been reported in PBMCs of RRMS (41), consistent with alteration of several scaRNAs and snoRNAs that guide posttranscriptional modifications of U2, U5, and U6 snRNAs (*SI Appendix*, Table S5). Since snRNAs are crucial regulators of alternative splicing, this strongly suggests disturbances in mRNA splicing, which has already been noted in MS (46). Indeed, activation of both T and B cells initiates global alternative splicing events in multiple genes of the NF-κB, mitogen-activated protein kinases and Rho GTPase signaling and cell proliferation pathways (47). Several splicing factors were found altered in MS (48), including factors that participate in the assembly of the aforementioned snRNAs in spliceosome units. Accordingly, our analysis of mRNA fragments

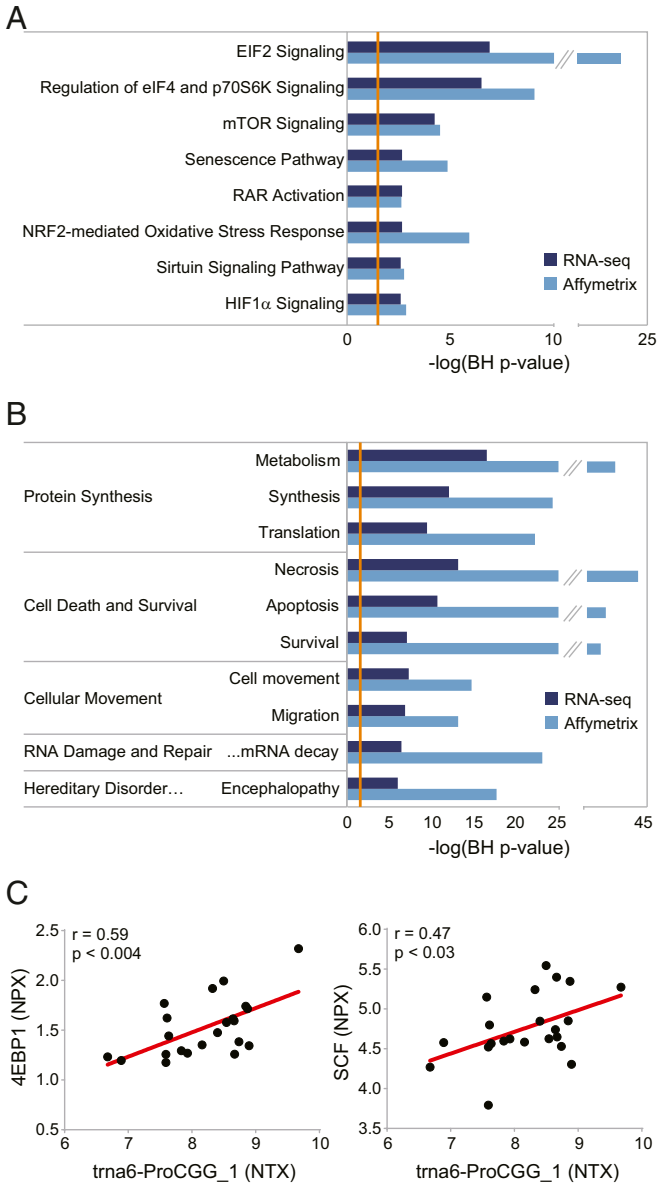

Fig. 6. Pathways and functions associating with MS status in CSF cells. CSF cell RNA sequencing of RRMS (relapse $n = 7$, remission $n = 4$) and NINDC ($n = 6$), as well as an independent CSF cell Affymetrix analysis (41) of RRMS (relapse $n = 12$, remission $n = 14$) and NINDC ($n = 18$). Transcripts associating with differentially expressed mRNAs (P value < 0.05) between RRMS versus NINDC were analyzed using IPA. (*Top*) (*A*) Canonical pathways and (*B*) diseases and functions (noncancer) comprising 10 molecules minimum. The $-\log_{10}$ of the Benjamini–Hochberg-corrected P value is provided on the x-axis, and the threshold for significance is indicated by the orange line. Default IPA analysis settings were used. Pearson correlations for normalized protein levels (NPX) of (*C*) 4EBP1, and SCF measured using a proteomic immunoassay (42) with normalized transcript levels (NTX) of tRNA6-ProCGG_1 ($n = 22$). See also Dataset S7.

also revealed decreased levels of transcripts deriving from two splicing factors, *SNRPB* and *RBFOX2*, in PBMCs of RRMS patients (Dataset S4). Altered RNA splicing in MS is consistent with increased levels of the long noncoding RNA *MALAT1*, affecting the expression of splicing factors *HNRNPF* and *HNRNPH1*, described in blood of RRMS patients (49). Interestingly, in our study, while *MALAT1*-associated small cytoplasmic RNA (mascRNA) was down-regulated in PBMCs of RRMS patients, levels of mascRNA were augmented in CSF cells in RRMS compared to controls (Dataset S4).

Alterations in alternative splicing mechanisms are further supported by the observed changes of snoRNAs, which exert noncanonical functions in mRNA processing (51, 52). Most of the sdRNAs exhibited down-regulation in PBMCs of RRMS compared to controls, which is in agreement with previous studies reporting predominant down-regulation of snoRNAs in $CD3^+$ T cells and PBMCs of MS patients (7). Notably, similar to the snRNA profile, these sdRNAs demonstrated the opposite pattern in CSF cells compared to PBMCs, with up-regulation in CSF cells in RRMS compared to controls, particularly during the relapse phase. Such a pattern was observed for several *U22* locus sdRNAs, including SNORD27, previously shown to regulate alternative splicing and to activate silent exons (50), thereby potentially contributing to the splicing defects implicated in MS. Notably, the majority of snoRNAs are encoded inside the introns of protein-coding genes, and their expression may be altered because of frequent intron retention due to splicing impairment. Finally, altered alternative splicing is also concordant with changes in miRNAs that can target alternative splicing factors. For example, miR-181a-5p, found up-regulated in CSF cells of RRMS patients, targets a member of the serine/arginine (SR)-rich family of splicing factor, SRSF7 (51). Overall, we show accumulating evidence from different sncRNA classes for aberrant alternative splicing mechanisms in MS.

Other dysregulated snoRNAs exert their canonical function by assisting with rRNA modifications essential for accurate ribosome function. Elevated levels of misprocessed 18S and 28S rRNAs have previously been reported in RRMS (25). The majority of detected sdRNAs are encoded inside structural ribosomal proteins, elongation factors, and translational regulators (*SI Appendix*, Table S5) (52, 53) controlled by the mTOR pathway (54). Since the transcription of such genes is activated when intensive protein production is required, the detected sdRNA alterations may reflect global changes in expression of translational machinery genes. Accordingly, our protein-coding RNA-sequencing analysis and previous independent data (41) implicate EIF2 signaling as the top enriched canonical pathway, together with changes in many ribosomal structural proteins and translational initiation factors in CSF cells of RRMS compared to controls.

Global changes in translation in RRMS patients are further supported by strong alterations of tRFs. Most of the Lys, Glu, Pro, His, and Ala tRFs were found up-regulated in CSF cells from RRMS compared to controls. Additionally, Met, Cys, Gly, and Val tRFs displayed robust up-regulation in CSF cells in RRMS as well as during the relapse phase. Similar to snRNAs and sdRNAs, tRFs changes in PBMCs exhibited the opposite direction (i.e., the majority of tRFs displayed down-regulation in PBMCs of RRMS patients). We observed specifically elevated levels of 5′-half tRFs that can target translation initiation machinery and inhibit translation (55) in response to stress conditions in CSF cells of RRMS patients. Elevated levels of specific tRFs in CSF cells may reflect adaptation to specific inflammatory conditions (56, 57) that initiate changes in protein profile synthesis and abundancy. It may also be a compensatory mechanism for excessively activated translation in RRMS.

The changes in tRFs, sdRNAs, and snRNAs may be linked to changes in mTOR activity known to facilitate cellular growth and proliferation. Indeed, in our study, the analysis of mRNAs in CSF cells implicated eIF4 and ribosomal protein S6 kinase 1 (S6K1/p70S6K) signaling as well as mTOR signaling among the most significant canonical pathways. One of the mTOR complexes, mTORC1, promotes mRNA translation and elongation through S6K1 and eIF4E-binding protein 1 as well as by increasing rRNA and tRNA transcription (58). Moreover, numerous differentially expressed tRFs from CSF cells correlated with CSF levels of 4E-BP1 and SCF. Both mTOR-dependent as well as SCF-dependent 4E-BP1 phosphorylation result in its release from eIF4E, leading to initiation of protein translation (59). Some evidence also

suggests the involvement of the mTORC1 complex in U-snRNP biogenesis (60). Additionally, we revealed in CSF cells alterations in metabolic pathways, such as the sirtuin signaling pathway, oxidative stress response, and hypoxia-inducible factor 1α (HIF1α) signaling in RRMS patients, that are all mediated by mTOR pathway (61). Taken together, the striking up-regulation of all of the above classes of sncRNAs in CSF cells, particularly in the relapse phase, is consistent with activation of mTOR signaling in activated and proliferating cells enriched in the target organ. In line with this, antigen recognition triggers mTOR signaling via the PI3K-Akt pathway and directs differentiation of naïve T cells into T_H1, T_H2, and T_H17 cells but inhibits differentiation of T_{REG} cells (61, 62). Increased levels of leptin, a hormone that activates mTOR signaling (63), has been reported in the CSF of RRMS patients, where leptin levels correlated with a reduced number of T_{REGS} (64). Additionally, the hyporesponsiveness of T_{REGS} from RRMS patients in vitro and in vivo is associated with activation of the leptin-mTOR metabolic pathway (65).

It is difficult to speculate to what degree the changes we observed are explained by changes occurring in encephalitogenic cells, enriched in the CSF compartment, and what is due to regulatory mechanisms in the larger population of nonencephalitogenic cells mainly located in the blood compartment. Another level of complexity relates to the temporal dynamics in the regulation of immune cells during the course of MS. For example, autoproliferation of bona fide encephalitogenic T and B cell clones is down-regulated in blood from MS patients in relapse compared to remission (66). Nevertheless, the identified changes in components of snRNA-mediated splicing machinery in PBMCs substantiate previously described alternative splicing disturbances in peripheral blood of MS patients and collectively concur to general disturbances of these processes in immune cells of MS patients (46) (Fig. 7). Conversely, changes in snoRNA- and tRNA-mediated mRNA translation mechanisms were more conspicuous in CSF cells. In MS, CSF cells preferentially include CCR7-expressing memory $CD4^+$ T cells, characterized by up-regulation of genes involved in T cell activation as opposed to down-regulation of genes associated with naïve cell state (41, 45, 67). Our observations are in accordance with a recent single-cell study comparing CSF cells and blood cells of MS patients during relapse (45). In blood cells, they demonstrated an increased transcriptional diversity compared to CSF cells, reflected by an increased proportion of differentially expressed genes across different cell clusters, while CSF cells show an up-regulation of cell cycle genes such as CCNC and Cyclin-C (45). In addition, most of the altered snRNAs, sdRNAs, and tRFs had a tendency of being decreased in PBMCs but increased in CSF cells of RRMS compared to INDC, which comprised systemic lupus erythematosus (SLE) patients (Figs. 3 and 4). Therefore, one can speculate that while in RRMS patients, there is an enrichment of activated proliferating cells with activated mTOR in the CSF compartment (Fig. 7), in SLE patients they may be directed to other organs.

In contrast to most sncRNAs, miRNAs did not display divergent changes between periphery and CNS. This observation supports the notion that inflammation triggers expression of miRNAs in multiple cell types, although the outcome of this up-regulation will strongly depend on the target mRNA content of the host cell. Interestingly, although miRNAs have been the most thoroughly studied sncRNA class to date, differentially expressed miRNAs constitute only a fraction of the altered sncRNAs in MS. Most of the differentially expressed miRNAs were detected in CSF cells during RRMS relapses, with a similar pattern across other compartments. Many of these miRNAs have previously been found to be up-regulated in peripheral immune cells from MS patients, that is, PBMCs and blood cells (e.g., miR-125a-5p, miR-146a-5p, miR-155–5p, miR-362–5p, and let-7d-5p) and $CD4^+$ T cells (miR-155–5p, let-7i-5p, and miR-486–5p) (7). Additionally, several miRNAs up-regulated in CSF cells in relapse,

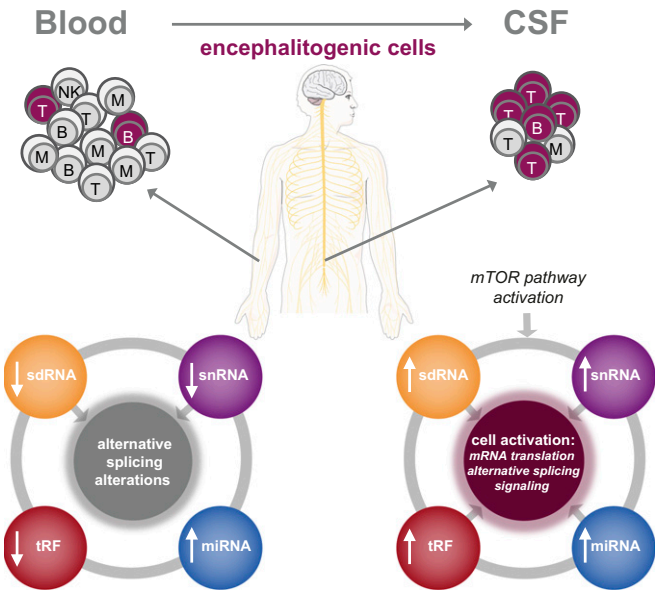

Fig. 7. Schematic overview of potential mechanisms of sncRNAs in the immunopathology of MS. Most differentially expressed classes of sncRNAs identified in peripheral blood mononuclear and CSF cells in this study include miRNAs, tRFs, and both full-length and fragments of snRNAs and sdRNAs, with white arrows indicating the direction of a change in MS patients. Cellular mechanisms implicated by differentially expressed sncRNAs in blood and CSF cells, with the latter being enriched in encephalitogenic cells, are outlined in middle circles, and support from a specific class of sncRNA is indicated by gray arrows.

compared to remission, have also been found dysregulated in the CNS tissue of MS patients: in inactive lesions (miR-155–5p, miR-30d-5p, and miR-532–5p), active lesions (miR-146b-5p, miR-320a, miR-142–5p, and miR-21–3p), demyelinated hippocampi (miR-30d-5p and let-7f-5p), and cell-free CSF (miR-21–3p and miR-191–5p) (7). Altogether, these findings suggest that infiltrating immune cells are likely the main cellular source of these CNS-detected miRNAs, although resident CNS cells might be an additional source. Interestingly, IPA analysis of the predicted targets of differentially expressed miRNA between relapse and remission unveiled TGF-β signaling as the most significant pathway. This is in line with previous studies suggesting miRNA-mediated alterations of TGF-β signaling, implicated in differentiation of both T_{REG} and T_H17 lineages, in MS (7, 68). Multiple detected miRNAs have been shown to target TGF-β signaling, including relapse-associated miR-21–3p, known to target RBPMS (69), which regulates TGF-β signaling by increasing transcriptional activity of Smad2/3 (70). Another example is miR-92a, also up-regulated in CSF cells during RRMS relapses, which targets SP1 (71) and has been shown to interact with Smad2/3/4 (72). Together with previous studies (7, 68), our findings position TGF-β signaling as a pivotal mechanism in the immunopathogenesis of MS.

In conclusion, our study demonstrates prominent cellular changes in several classes of sncRNAs with substantial changes correlating with disease status (RRMS versus NINDC) and disease activity (relapse versus remission), likely reflecting enrichment of activated encephalitogenic cells in the target organ. Contrasting differentially regulated sncRNA species between the blood and CSF compartments and between relapse and remission highlights the importance of sncRNA-mediated mechanisms—in particular, alternative splicing, mRNA degradation, and translation—in shaping up the transcriptome and function of pathogenic cells in MS.

Materials and Methods

For detailed information and protocols, see *SI Appendix*.

Patients. A total of 23 RRMS and 5 SPMS patients, 5 INDCs, and 11 NINDCs (a total of 44 samples) were included, of which matching PBMC, plasma, CSF cells, and cell-free CSF samples were used. Detailed cohort characteristics are presented in *SI Appendix*, Table S1. The study was approved by the Regional Ethical Board (2009/2107–31/2). All patients signed the informed consent.

Sample Preparation.

Preparation of cell-free CSF and CSF cells. CSF was centrifuged immediately after lumbar puncture at 440 g for 10 min at room temperature (RT) to separate cells from supernatants, then stored at −80 °C. For details, see *SI Appendix*.

Plasma preparation. Blood was centrifuged at 1,500 *g* for 15 min at RT. The plasma phase was stored at −80 °C.

Preparation of peripheral blood cells. Blood samples were centrifuged at 1,500 *g* for 15 min at RT. The plasma layer was aspirated, and the cell layer was washed with 15 mL phosphate-buffered saline (PBS) and centrifuged at 300 g for 15 min at RT. The pellet was resuspended in 3 mL PBS, centrifuged at 300 g for 10 min at RT followed by aspiration of supernatants, and then stored at –80 °C. For details, see *SI Appendix*.

RNA Extraction.

RNA isolation from cell-free CSF and plasma samples. RNA was isolated from 300 μL of plasma or CSF using miRCURY RNA isolation kit for biofluids (Exiqon). RNA was eluted with 15 μL and 20 μL of RNase-free water for CSF and plasma samples, respectively, and stored at −80 °C. For details, see *SI Appendix*.

RNA isolation from CSF cells and PBMCs. CSF cells and PBMCs were resuspended in 900 μl QIAzol Lysis Reagent (Qiagen) and 180 μL of Chloroform (Merck). RNA was isolated using miRNeasy micro kit (Qiagen). RNA was eluted with 15 μL and 40 μL of RNase-free water for CSF cell and PBMC samples, respectively, and stored at −80 °C. For details, see *SI Appendix*.

Library Preparation and Sequencing.

sncRNA library preparation and sequencing. Library preparation for all 44 samples from each compartment (PBMCs, plasma, CSF cells, and cell-free CSF) mostly followed the described protocol (32, 33). Libraries were pooled for each compartment and purified. Automatic size selection was performed using the Pippin Prep (Sage Science, Inc.). Each pool was sequenced on two lanes of Illumina HiSeq2500 single-end 1 × 51 bp (*SI Appendix*, Fig. S9*A*). Additionally, the CSF cell samples pool without Pippin Prep size selection was sequenced 1 × 101 bp single-end on an Illumina HiSeq2500 (*SI Appendix*, Fig. S9*C*). For details, see *SI Appendix*.

Technical replication. PBMCs, plasma, CSF cells, and cell-free CSF samples ($n = 3$ per compartment and $n = 12$ in total) were chosen from the same cohort; libraries were prepared following the above-described protocol and sequenced 1 × 101 bp single-end on an Illumina HiSeq2500 Rapid mode lane (*SI Appendix*, Fig. S9*B*).

CSF cells library preparation and total RNA sequencing. Libraries were generated from CSF cells of RRMS (relapse $n = 7$ and remission $n = 4$) and NINDC ($n = 6$) with SMARTer stranded total RNA-seq Pico input mammalian kit (Clontech Laboratories) and sequenced 2 × 151 bp paired-end on Illumina NovaSeq6000 (*SI Appendix*, Fig. S9*D*).

Data Analysis.

Preprocessing and read alignment. Preprocessing and alignment of reads was done according to Hagemann–Jensen et al. (33). For details, see *SI Appendix*.

Length distribution analysis. To investigate length distribution of sncRNAs, sequences in the final preprocessed BAM files were filtered based on requiring 50% reciprocal overlap with selected biotypes using the BEDTools intersect function.

Transcript filter. Transcripts with less than 2 UMIs in more than 80% of individual samples per contrasted group (i.e., RRMS, NINDC, relapse, and remission) were filtered out. For details, see *SI Appendix*.

Normalization. Filtered transcripts were normalized with trimmed mean of M values method. For details, see *SI Appendix*.

Detection of differentially expressed transcripts. Differential expression analysis was performed utilizing the limma package. The linear model for the first analysis (contrast RRMS–NINDC) included the following: disease status (NINDC, INDC, RRMS, and SPMS), sex, age, and repeated individual (one SPMS patient was sampled twice 1 y apart), and the second analysis (contrast relapse–remission) included RRMS status (relapse and remission), sex, and age. For details, see *SI Appendix*.

Heatmaps. Hestat Heatmaps illustrate Z-score (fitted, normalized log2-transformed UMI counts/million [lcmp]) values from transcripts filtered based on reported (Benjamini–Hochberg corrected) P value threshold < 0.01 and were centered and scaled within each compartment.

tRF analysis using MINTmap. Trimmed reads were mapped to the tRNA reference set (tRNA space) using MINTmap (40). For details, see *SI Appendix*.

CSF cells total RNA sequencing analysis. CSF cells total RNA libraries ($n = 17$) were preprocessed with TrimGalore, mapped with STAR against hg38, and annotated using featureCounts with Ensemble GRCh38. Differential expression analysis was performed with DESeq2. For details, see *SI Appendix*.

Microarray data. Gene expression profiling was performed on paired PBMC and CSF samples of RRMS patients (relapse $n = 12$ and remission $n = 14$), without immunomodulatory treatment, and NINDC ($n = 18$) using Human Genome U133 plus 2.0 arrays (Affymetrix). For details, see *SI Appendix*.

Gene ontology analyses. Gene ontology analysis was performed using IPA (Qiagen) to generate canonical pathways and diseases and functions. For details, see *SI Appendix*.

Data Availability. The RNA-seq data used for sncRNA analyses is available in the Swedish National Data Service (https://doi.org/10.5878/c1mq-9r62) (73). Anonymized RNA-seq data have been deposited in the Swedish National Data Service.

ACKNOWLEDGMENTS. This work was supported by the Swedish Research Council (Vetenskapsrådet), the Swedish Association for Persons with Neurological Disabilities, the Swedish Brain Foundation, the Swedish MS Foundation, the Stockholm County Council (ALF project), AstraZeneca (AstraZeneca-Science for Life Laboratory collaboration), the European Union's Horizon 2020 research innovation programme (Grant Agreement No. 733161), and the European Research Council (grant Agreement No. 818170), the Knut and Alice Wallenberg Foundation, and the Swedish Society for Medical Research. We acknowledge the National Genomics Infrastructure in Stockholm, funded by Science for Life Laboratory, the Knut and Alice Wallenberg Foundation and Vetenskapsrådet, and Swedish National Infrastructure for Computing (SNIC)/Uppsala Multidisciplinary Center for Advanced Computational Science. We also acknowledge input on the initial analysis from Dr. Francesco Marabita, input on writing from Dr. Lara Kular, and computational input from Dr. Christoph Ziegenhain.

1. M. Filippi *et al.*, Multiple sclerosis. *Nat. Rev. Dis. Primers* **4**, 43 (2018).
2. T. Olsson, L. F. Barcellos, L. Alfredsson, Interactions between genetic, lifestyle and environmental risk factors for multiple sclerosis. *Nat. Rev. Neurol.* **13**, 25–36 (2017).
3. International Multiple Sclerosis Genetics Consortium, Multiple sclerosis genomic map implicates peripheral immune cells and microglia in susceptibility. *Science* **365**, eaav7188 (2019).
4. K. V. Morris, J. S. Mattick, The rise of regulatory RNA. *Nat. Rev. Genet.* **15**, 423–437 (2014).
5. B. M. Engels, G. Hutvagner, Principles and effects of microRNA-mediated post-transcriptional gene regulation. *Oncogene* **25**, 6163–6169 (2006).
6. M. Mittelbrunn *et al.*, Unidirectional transfer of microRNA-loaded exosomes from T cells to antigen-presenting cells. *Nat. Commun.* **2**, 282 (2011).
7. E. Piket, G. Y. Zheleznyakova, L. Kular, M. Jagodic, Small non-coding RNAs as important players, biomarkers and therapeutic targets in multiple sclerosis: A comprehensive overview. *J. Autoimmun.* **101**, 17–25 (2019).
8. B. Shademan *et al.*, Investigation of the miRNA146a and miRNA155 gene expression levels in patients with multiple sclerosis. *J. Clin. Neurosci.* **78**, 189–193 (2020).
9. L. Fritsche *et al.*, MicroRNA profiles of MS gray matter lesions identify modulators of the synaptic protein synaptotagmin-7. *Brain Pathol.* **30**, 524–540 (2020).
10. Z. H. Li *et al.*, Let-7f-5p suppresses Th17 differentiation via targeting STAT3 in multiple sclerosis. *Aging (Albany NY)* **11**, 4463–4477 (2019).
11. O. Perdaens, H. A. Dang, L. D'Auria, V. van Pesch, CSF microRNAs discriminate MS activity and share similarity to other neuroinflammatory disorders. *Neurol. Neuroimmunol. Neuroinflammation* **7**, e673 (2020).
12. B. Huang *et al.*, miR-142-3p restricts cAMP production in CD4+CD25- T cells and CD4+CD25+ TREG cells by targeting AC9 mRNA. *EMBO Rep.* **10**, 180–185 (2009).
13. G. Murugaiyan, V. Beynon, A. Mittal, N. Joller, H. L. Weiner, Silencing microRNA-155 ameliorates experimental autoimmune encephalomyelitis. *J. Immunol.* **187**, 2213–2221 (2011).
14. R. Liu *et al.*, MicroRNA-15b suppresses Th17 differentiation and is associated with pathogenesis of multiple sclerosis by targeting *O*-GlcNAc transferase. *J. Immunol.* **198**, 2626–2639 (2017).
15. P. Bergman *et al.*, Circulating miR-150 in CSF is a novel candidate biomarker for multiple sclerosis. *Neurol. Neuroimmunol. Neuroinflammation* **3**, e219 (2016).
16. E. Quintana *et al.*, miRNAs in cerebrospinal fluid identify patients with MS and specifically those with lipid-specific oligoclonal IgM bands. *Mult. Scler.* **23**, 1716–1726 (2017).
17. R. Gandhi *et al.*, Circulating microRNAs as biomarkers for disease staging in multiple sclerosis. *Ann. Neurol.* **73**, 729–740 (2013).
18. M. Jernås *et al.*, MicroRNA regulate immune pathways in T-cells in multiple sclerosis (MS). *BMC Immunol.* **14**, 32 (2013).

19. H. Irizar *et al.*, Identification of ncRNAs as potential therapeutic targets in multiple sclerosis through differential ncRNA–mRNA network analysis. *BMC Genomics* **16**, 250 (2015).
20. M. Muñoz-Culla *et al.*, SncRNA (microRNA &snoRNA) opposite expression pattern found in multiple sclerosis relapse and remission is sex dependent. *Sci. Rep.* **6**, 20126 (2016).
21. C. Ender *et al.*, A human snoRNA with microRNA-like functions. *Mol. Cell* **32**, 519–528 (2008).
22. A. M. Burroughs *et al.*, Deep-sequencing of human Argonaute-associated small RNAs provides insight into miRNA sorting and reveals Argonaute association with RNA fragments of diverse origin. *RNA Biol.* **8**, 158–177 (2011).
23. F. Dupuis-Sandoval, M. Poirier, M. S. Scott, The emerging landscape of small nucleolar RNAs in cell biology. *Wiley Interdiscip. Rev. RNA* **6**, 381–397 (2015).
24. M. Falaleeva, S. Stamm, Processing of snoRNAs as a new source of regulatory non-coding RNAs: snoRNA fragments form a new class of functional RNAs. *BioEssays* **35**, 46–54 (2013).
25. C. F. Spurlock 3rd *et al.*, Defective structural RNA processing in relapsing-remitting multiple sclerosis. *Genome Biol.* **16**, 58 (2015).
26. M. P. Kowalski, T. Krude, Functional roles of non-coding Y RNAs. *Int. J. Biochem. Cell Biol.* **66**, 20–29 (2015).
27. P. Schimmel, The emerging complexity of the tRNA world: Mammalian tRNAs beyond protein synthesis. *Nat. Rev. Mol. Cell Biol.* **19**, 45–58 (2018).
28. P. Krishnan *et al.*, Genome-wide profiling of transfer RNAs and their role as novel prognostic markers for breast cancer. *Sci. Rep.* **6**, 32843 (2016).
29. M. C. Hogg *et al.*, Elevation in plasma tRNA fragments precede seizures in human epilepsy. *J. Clin. Invest.* **129**, 2946–2951 (2019).
30. L. Zhu, J. Ge, T. Li, Y. Shen, J. Guo, tRNA-derived fragments and tRNA halves: The new players in cancers. *Cancer Lett.* **452**, 31–37 (2019).
31. Q. Chen *et al.*, Sperm tsRNAs contribute to intergenerational inheritance of an acquired metabolic disorder. *Science* **351**, 397–400 (2016).
32. O. R. Faridani *et al.*, Single-cell sequencing of the small-RNA transcriptome. *Nat. Biotechnol.* **34**, 1264–1266 (2016).
33. M. Hagemann-Jensen, I. Abdullayev, R. Sandberg, O. R. Faridani, Small-seq for single-cell small-RNA sequencing. *Nat. Protoc.* **13**, 2407–2424 (2018).
34. R. Waller *et al.*, Small RNA sequencing of sporadic amyotrophic lateral sclerosis cerebrospinal fluid reveals differentially expressed miRNAs related to neural and glial activity. *Front. Neurosci.* **11**, 731 (2018).
35. P. M. Godoy *et al.*, Large differences in small RNA composition between human biofluids. *Cell Rep.* **25**, 1346–1358 (2018).
36. A. Yeri *et al.*, Total extracellular small RNA profiles from plasma, saliva, and urine of healthy subjects. *Sci. Rep.* **7**, 44061 (2017).
37. S. Srinivasan *et al.*, Small RNA sequencing across diverse biofluids identifies optimal methods for exRNA isolation. *Cell* **177**, 446–462.e16 (2019).
38. M. El-Mogy *et al.*, Diversity and signature of small RNA in different bodily fluids using next generation sequencing. *BMC Genomics* **19**, 408 (2018).
39. S. Griffiths-Jones, Annotating noncoding RNA genes. *Annu. Rev. Genomics Hum. Genet.* **8**, 279–298 (2007).
40. P. Loher, A. G. Telonis, I. Rigoutsos, MINTmap: Fast and exhaustive profiling of nuclear and mitochondrial tRNA fragments from short RNA-seq data. *Sci. Rep.* **7**, 41184 (2017).
41. B. Brynedal *et al.*, Gene expression profiling in multiple sclerosis: A disease of the central nervous system, but with relapses triggered in the periphery? *Neurobiol. Dis.* **37**, 613–621 (2010).
42. J. Huang *et al.*, Inflammation-related plasma and CSF biomarkers for multiple sclerosis. *Proc. Natl. Acad. Sci. U.S.A.* **117**, 12952–12960 (2020).
43. M. Stangel *et al.*, The utility of cerebrospinal fluid analysis in patients with multiple sclerosis. *Nat. Rev. Neurol.* **9**, 267–276 (2013).
44. P. Kivisäkk *et al.*, Natalizumab treatment is associated with peripheral sequestration of proinflammatory T cells. *Neurology* **72**, 1922–1930 (2009).
45. D. Schafflick *et al.*, Integrated single cell analysis of blood and cerebrospinal fluid leukocytes in multiple sclerosis. *Nat. Commun.* **11**, 247 (2020).
46. M. Hecker *et al.*, Aberrant expression of alternative splicing variants in multiple sclerosis–A systematic review. *Autoimmun. Rev.* **18**, 721–732 (2019).
47. N. M. Martinez, K. W. Lynch, Control of alternative splicing in immune responses: Many regulators, many predictions, much still to learn. *Immunol. Rev.* **253**, 216–236 (2013).
48. E. M. Paraboschi *et al.*, Meta-analysis of multiple sclerosis microarray data reveals dysregulation in RNA splicing regulatory genes. *Int. J. Mol. Sci.* **16**, 23463–23481 (2015).
49. G. Cardamone *et al.*, Not only cancer: The long non-coding RNA MALAT1 affects the repertoire of alternatively spliced transcripts and circular RNAs in multiple sclerosis. *Hum. Mol. Genet.* **28**, 1414–1428 (2019).
50. M. Falaleeva *et al.*, Dual function of C/D box small nucleolar RNAs in rRNA modification and alternative pre-mRNA splicing. *Proc. Natl. Acad. Sci. U.S.A.* **113**, E1625–E1634 (2016).
51. J. Boguslawska *et al.*, microRNAs target SRSF7 splicing factor to modulate the expression of osteopontin splice variants in renal cancer cells. *Gene* **595**, 142–149 (2016).
52. E. S. Maxwell, M. J. Fournier, The small nucleolar RNAs. *Annu. Rev. Biochem.* **64**, 897–934 (1995).
53. C. M. Smith, J. A. Steitz, Classification of gas5 as a multi-small-nucleolar-RNA (snoRNA) host gene and a member of the 5′-terminal oligopyrimidine gene family reveals common features of snoRNA host genes. *Mol. Cell. Biol.* **18**, 6897–6909 (1998).
54. O. Meyuhas, Synthesis of the translational apparatus is regulated at the translational level. *Eur. J. Biochem.* **267**, 6321–6330 (2000).
55. P. Ivanov, M. M. Emara, J. Villen, S. P. Gygi, P. Anderson, Angiogenin-induced tRNA fragments inhibit translation initiation. *Mol. Cell* **43**, 613–623 (2011).
56. M. Saikia *et al.*, Genome-wide identification and quantitative analysis of cleaved tRNA fragments induced by cellular stress. *J. Biol. Chem.* **287**, 42708–42725 (2012).
57. M. Torrent, G. Chalancon, N. S. de Groot, A. Wuster, M. Madan Babu, Cells alter their tRNA abundance to selectively regulate protein synthesis during stress conditions. *Sci. Signal.* **11**, eaat6409 (2018).
58. M. Laplante, D. M. Sabatini, mTOR signaling in growth control and disease. *Cell* **149**, 274–293 (2012).
59. N. Hay, N. Sonenberg, Upstream and downstream of mTOR. *Genes Dev.* **18**, 1926–1945 (2004).
60. O. J. Gruss, R. Meduri, M. Schilling, U. Fischer, UsnRNP biogenesis: Mechanisms and regulation. *Chromosoma* **126**, 577–593 (2017).
61. H. Chi, Regulation and function of mTOR signalling in T cell fate decisions. *Nat. Rev. Immunol.* **12**, 325–338 (2012).
62. C. Procaccini *et al.*, An oscillatory switch in mTOR kinase activity sets regulatory T cell responsiveness. *Immunity* **33**, 929–941 (2010).
63. V. De Rosa *et al.*, A key role of leptin in the control of regulatory T cell proliferation. *Immunity* **26**, 241–255 (2007).
64. G. Matarese *et al.*, Leptin increase in multiple sclerosis associates with reduced number of CD4(+)CD25+ regulatory T cells. *Proc. Natl. Acad. Sci. U.S.A.* **102**, 5150–5155 (2005).
65. F. Carbone *et al.*, Regulatory T cell proliferative potential is impaired in human autoimmune disease. *Nat. Med.* **20**, 69–74 (2014).
66. I. Jelcic *et al.*, Memory B cells activate brain-homing, autoreactive $CD4^+$ T cells in multiple sclerosis. *Cell* **175**, 85–100.e23 (2018).
67. B. Fritzsching *et al.*, Intracerebral human regulatory T cells: Analysis of CD4+ CD25+ FOXP3+ T cells in brain lesions and cerebrospinal fluid of multiple sclerosis patients. *PLoS One* **6**, e17988 (2011).
68. M. E. Severin *et al.*, MicroRNAs targeting TGFβ signalling underlie the regulatory T cell defect in multiple sclerosis. *Brain* **139**, 1747–1761 (2016).
69. N. Hou *et al.*, Inhibition of microRNA-21-3p suppresses proliferation as well as invasion and induces apoptosis by targeting RNA-binding protein with multiple splicing through Smad4/extra cellular signal-regulated protein kinase signalling pathway in human colorectal cancer HCT116 cells. *Clin. Exp. Pharmacol. Physiol.* **45**, 729–741 (2018).
70. Y. Sun *et al.*, Potentiation of Smad-mediated transcriptional activation by the RNA-binding protein RBPMS. *Nucleic Acids Res.* **34**, 6314–6326 (2006).
71. A. Kulyté *et al.*, Additive effects of microRNAs and transcription factors on CCL2 production in human white adipose tissue. *Diabetes* **63**, 1248–1258 (2014).
72. X. H. Feng, X. Lin, R. Derynck, Smad2, Smad3 and Smad4 cooperate with Sp1 to induce p15(Ink4B) transcription in response to TGF-beta. *EMBO J.* **19**, 5178–5193 (2000).
73. G. Zheleznyakova, E. Piket, M. Needhamsen, M. Jagodic, Small non-coding RNA profiling across cellular and biofluid compartments and their implications for multiple sclerosis immunopathology (Version 1.0) [Data set]. Swedish National Data Service (SND). https://doi.org/10.5878/c1mq-9r62. Deposited 8 April 2021.